Advanced non-destructive techniques for the diagnosis of historic buildings: The Loka-Hteik-Pan temple in Bagan

Advanced non-destructive techniques for the diagnosis of historic buildings: the Loka-Hteik-Pan temple in Bagan

Erik Costamagna[a,*], Mario Santana Quintero[a], Nicoletta Bianchini[b], Nuno Mendes[b], Paulo B. Lourenço[b], Su Su[c], Yin Min Paik[c], Aungzaw Min[d]

[a] *Carleton Immersive Media Studio, Carleton University, Ottawa, Canada*
[b] *ISISE, Institute of Science and Innovation for Bio-Sustainability (IB-S), University of Minho, Guimarães, Portugal*
[c] *Mandalay Technological University, Mandalay, Myanmar*
[d] *Department of Archaeology and National Museum, Bagan, Myanmar*

Abstract

The archaeological site of Old Bagan, located in the centre of Myanmar, is one of the most remarkable and ancient Asian site with over three thousand monuments, scattered in an area of about eighty square kilometers. The site was hit in 2016 by the last of a series of earthquakes. The Loka-Hteik-Pan is a hollow-core temple featured by a small elegant curvilinear tower. It was significantly damaged by the event, losing the upper part of the tower, as many other temples of the area. Emergencies like seismic events generally require quick responses and targeted solutions. When a built area is involved, damaged buildings need structural assessments with a special focus on space and time occupancy, without compromising the reliability of the results. A workflow for data acquisition and analysis is proposed, using non-destructive techniques to evaluate the materials performances and measure spatial changes over times. Deformation analysis is performed on LiDAR data, acquired prior and after the earthquake, with the goal of measuring small changes occurred in the wall surfaces. The preliminary results of the tests are presented with the purpose to provide a knowledge base, useful to guide the interventions for preserving the monument and its heritage.

Keywords: Cultural heritage; Non-Destructive Testing; Terrestrial Laser Scanning; Point Cloud; Deformation Analysis;

1. Introduction

Tangible cultural heritage like architectural and archaeological ones are a testimony of cultural values, shared by people during a period of time, which need to be preserved in order to be passed down to future generations. Such values are carried not only by the appearance of the object but also by the integrity of all its components [1]. The documentation process is a multidisciplinary activity involving a broad range of sciences among which geomatics is essential to relate and integrate all the sparse information pieces in a comprehensive description of the whole building system [2].

Non-Destructive Testing (NDT) is a broad collection of methods for the examination and analysis of objects and systems without impairing them or affecting their integrity. They are widely used in civil engineering for testing the performances of new structures as well for the damage monitoring in old constructions. Such techniques include the sonic transmission method, used to test the elastic properties in order to acquire information about the structural performance of the materials and guide future interventions on the building. Nowadays geomatics methods like topography and photogrammetry also allow a contactless non-invasive acquisition of metric information from

*Corresponding author, present address: Department of Architecture and Design (DAD), Politecnico di Torino, Italy

Email addresses: erik.costamagna@carleton.ca (Erik Costamagna), mario.santana@carleton.ca (Mario Santana Quintero), nicoletta.bianchini@gmail.com (Nicoletta Bianchini), nunomendes@civil.uminho.pt (Nuno Mendes), pbl@civil.uminho.pt (Paulo B. Lourenço), susu.bagan2017@gmail.com (Su Su), yinminpaik@mtu.edu.mm (Yin Min Paik), komindelhi06@gmail.com (Aungzaw Min)

objects. Light Detection and Ranging (LiDAR) is a promising topographic technique which has been extensively used for structural monitoring. Its main advantage is the possibility to acquire automatically and massively high detailed measures from objects. Later the development in electronics reduced significantly the size and cost of such sensors, while developments of algorithms for spatial analysis and manipulation automated the possibility to extract useful information from the acquired data. These advancement boosted the application of such technique to a larger set of purposes such as deformation detection and measurement, potentially reducing the cost of human intervention[3].

2. Research aim

The presented research was conducted in 2018 as a collaboration between Carleton University, Mandalay Technological University and the Department of Archaeology and National Museums of Myanmar. It involved a series of field activities, workshops and conferences aimed to disseminate the knowledge about Bagan archaeological site by using innovative techniques for the documentation and conservation of its cultural values. The site includes thousands of religious buildings and was affected by a series of seismic events over time, the last of them in 2016. The object of study is one of the temple which has been studied over time and was damaged by the last earthquake which destroyed the upper part of the roof. The goal of this research is to show the effectiveness of advanced non-destructive techniques that can be deployed after an earthquake for a fast and reliable assessment of seismic damages and guidance for the interventions to be put in place.

3. Diagnostic techniques

3.1. Non-destructive testing

One of the older and simpler systems for evaluating the structural heath of a building is the direct visual inspection, which requires the physical access to all the building parts and it is strongly influenced by subjectivity [4]. On the other hand, non-destructive techniques allow to measure physical properties of the materials which are crucial to determine the building seismic response. One of these techniques is sonic pulse velocity testing, which can be used to estimate the elastic properties of materials. This type of test is based on the propagation of waves inside the materials caused by an impulsive force. The velocity and the time spent to receive the signal, generated from the waves, can be read between the thickness of the internal and external surfaces of the walls (direct sonic tests) or along the same surface (indirect tests) at a specific distance. While visual inspection gives a general overview of the observed state of damage along the structure, the sonic tests are performed with the goal of evaluating the elastic properties through the reading of the velocity waves. Depicting the variation of velocity in different locations of the temple may correspond to an increase or decrease of the elastic properties due to internal cracks, deteriorations and/or detachments.

3.2. Point cloud processing

Registration

LiDAR is a ranging technology for automatically and randomly extracting massive amount of measures from objects, resulting in a dense collection of points called point cloud. After filtering out systematic errors and outliers, point clouds can be considered as an highly detailed sample of a spatial feature, with a certain amount of random error called noise. Commonly point cloud noise is calculated as roughness, which is the deviation from a local plane. The accuracy of the sample is commonly given as spatial density or point spacing. When surveying a 3-dimensional feature multiple scans of the same scene need to be acquired and consequently aligned together. This process, called registration, is the computation of the fixed-scale geometric transformation, necessary to reference multiple scans in the same Coordinate Reference System (CRS). It can be done either by using a different reference system, independently defined by a set of Ground Control Points (GCPs), or using the same CRS of one of the scan positions. The latter, known as co-registration, does not require additional sensory while an high overlap between the scans is necessary to avoid systematic errors [5].

Pre-determined associations between features from the two sets can be used for computing the parameters of the transformation. In this approach,

called target-based registration, markers are used as tie points for the scans registration. In the cloud to cloud approach no prior knowledge about correspondences is given, these are automatically found using points coordinates minimizing the reciprocal distances between the clouds. Intensive distance computations on point clouds are improved using indexing structures like the octree [6], which is an efficient hierarchical data structure based on a regular space decomposition [1]. A very popular algorithm for the cloud to cloud fine registration is the Iterative Closest Point (ICP) [7]. This algorithm selects a set of samples from one cloud and find point to point correspondences to neighbours in the other set. The point to point calculation method requires an high degree of overlap between the pairs and an uniform point density within the scans.

Spatial analysis and interpolation

Development of algorithms for the analysis of spatial changes increased the effectiveness of using LiDAR techniques and potentially extended theirs application field for detecting and measuring spatio-temporal changes without any prior knowledge. Deformation analysis and change detection are the two main specialization of this topic, the former dealing with the binary problem of distinguish stable and unstable areas while the latter is focused on the accurate measurement of small changes, usually close to the instrument tolerance. Change detection techniques are usually applied to geosciences problems, where the co-registration of laser scans acquired in different epochs on the base of manually identified stable areas can be a challenge. Automatic co-registration of laser scans and change detection are indeed mutually dependent: registration of scans affected by spatial changes requires robustness against outliers (unstable areas), that is the sampling of tie points only from stable areas. This issue is addressed either using sequential [8] and combinatory approaches [9]. Identification of stable areas where to sample tie points for the laser scans registration is usually less problematic when the application field involves buildings, whose 3D models are usually featured by parametrized surfaces. In the construction field deformation is usually computed as a deviation of the acquired data from geometric primitives and out-of-plane tests are also common to check the deflection of wall surfaces from vertical [10] [11].

One of the first cloud comparison method developed was the cloud to model (or mesh) (C2M) [12] which can be used to compare point sets to surfaces models. Surface reconstruction from unstructured point clouds is performed by interpolating the points, usually with patches resulting in a facet model called mesh. While several approaches exist to find the best surface fitting for a point set, uncertainties introduced by interpolation are difficult to quantify. Methods for the cloud to cloud (C2C) comparison have also been developed, computing distances along normal directions without performing a surface reconstruction of the whole point set, but rather approximating locally the surface. Least squares planes, Delaunay triangulations and quadric surfaces are some of the models used as local best approximation of a point set, depending on the roughness and the level of detail [13]. Brodu and Lague proposed a C2C method called Model to Model Multiscale Cloud Comparison (M3C2) [14] which addresses some of the limitations of the other C2C approaches. First of all the algorithm computes normals for the whole point cloud to be compared at different scales, choosing the surface fitting which minimizes the difference in normal orientation between neighbour points. Thereafter the normals direction is used to project the neighbour points, whose mean value represents the average position of the points along that direction, while the standard deviation measures the roughness of the sampled points. Cloud to cloud local distance is thus computed as the distance between the two mean values. The SD is calculated for both the clouds and the results, together with the registration error (if available), are used to estimate the uncertainty of each measured distance, giving a local level of confidence for the C2C comparison. A statistical method for determining significant changes with the C2M method has also been proposed and used to test C2M against M3C2 [9]. M3C2 method has been tested in remote sensing [15] and close-range applications [16] with positive results. Detection and measurement of changes between two (or more) point sets acquired in different times requires the two sets to be registered using in the same Coordinate Reference System (CRS). The po-

[1] Given a point set and a the smallest cubical bounding box containing it, the space within the box is divided recursively into 8 sub-cubes at each octree depth level till no points are contained or a minimum density level is reached.

tential presence of changes between the two sets poses the problem to exclude this bias from the computation of registration parameters. Automatic registration methods like ICP, which extract randomly tie points to be used for adjustment, can lead to misalignment if the deformation area is too large [13]. Most of the cited methods consider only displacements in one dimension, usually coincident with the normal vector. Registration methods like the Least Square 3D (LS3D) [17] have been used in geosciences applications for measuring deformation in the 3D space [18], given a prior knowledge about the areas subjected to change.

4. Data acquisition and analysis

4.1. Description of the temple and main interventions

The Loka-Hteik-Pan temple, numbered as 1580 by Pichard's Inventory [19], is a middle-size temple, built in 1113 A.D. in the south-western part of the old Bagan site (Myanmar). This temple is still nowadays one of the most remarkable example of Burmese and Buddhist Architecture, not only for its shape and function, but also because of the original paintings of Buddha's Life which are located on the inner surfaces of the temple.

The temple is an isolated structure of about $150\,m^2$, made of fired bricks, which can be divided into three spaces: the main chamber, which hosts the Buddha's statue, the antechamber and the entrance (Figure:1). The entrance and the antechamber are covered by two barrel vaults, while the main chamber hosts a cloister vault [21]. Shapes are massive and articulated by the sequence of several terraces up to the level of the Śikhara, a sort of curvilinear high tower characteristic of Indian and Burmese temples. The terraces are accessible via an internal and narrow staircase, dug in the thickness of external wall (more than 2.5 m). The Śikhara (Figure:1) is one architectural element with origin in the Indian architecture - it is a sort of curvilinear tower which offers a slender appearance to the temple [22].

Three perforated brick windows let some light enter into the main chamber and they are the unique way to light the interior. From the exterior, the windows are framed by ornamental portals, with characteristic details of the Buddhist art. The North façade has the entrance and it is marked by a portal, which presents a tympanum. Most of the external surfaces were covered by stucco carvings, applied directly on the outer layer of the masonry, mouldings sculptures or reliefs. Nowadays, only partial remaining parts of these carvings are still located on the surfaces.

From the 13th and 19th centuries, Loka-Hteik-Pan temple passed through several construction phases that are not well known.

Due to the numerous seismic events, which hit Central Myanmar during 20^{th} and 21^{th} centuries (See Figure 2), Loka-Hteik-Pan temple, as well as many other Bagan temples, underwent several structural and non-structural interventions. The most significant changes occurred after Bagan earthquake (1975), when locals funded heavy strengthening projects [23]. According to Pichard [19], "a reinforced concrete belt at the top of the walls" was inserted along the perimeter walls of the main chambers. This description does not represent the entire intervention that was made: three beams made of reinforced concrete, not continuous, were located at each corners of the main chamber and of the antechamber along the height of the structure. This work was supposed to be done in order to re-establish the connection between the walls.

Many portions of the portals and all the final parts of the pinnacles were rebuilt during the last century, using modern and industrial fired bricks. The Śikhara was restored several times and nowadays many of its bricks are not original, but newer and pasted through the use of cement based mortar. The original spire of the Śikhara disappeared; this element was repositioned with a new steel fastener after 1975 Earthquake, but it collapsed during the Chauk earthquake (2016). The spire was not replaced after this event and the highest part of the Śikhara, which did not collapse, was restored with the insertion of new bricks.

The frescoes were treated the first time in 1993, after the earthquake that hit Bagan in 1992. The paintings were cleaned against the action of the dust, using mechanical brushes and wet cleaning technique with chemical solvents. The last intervention on the mural paintings took place in 2015: liquid grout injection was employed to re-establish the adhesion of them on the walls.

4.2. Damage survey

The damage survey was evaluated through visual inspection in May 2018, aiming at updating the evaluation of the damage after the 2016 Chauk

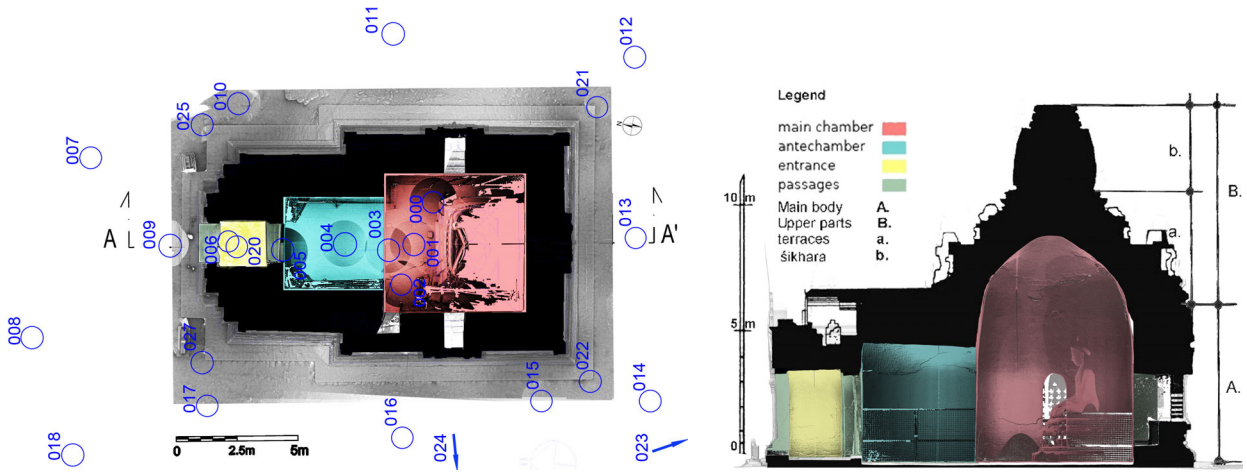

Figure 1: Loka-Hteik-Pan: vertical section and ground level plan with the scan locations from 2018. Source: updated from [19]

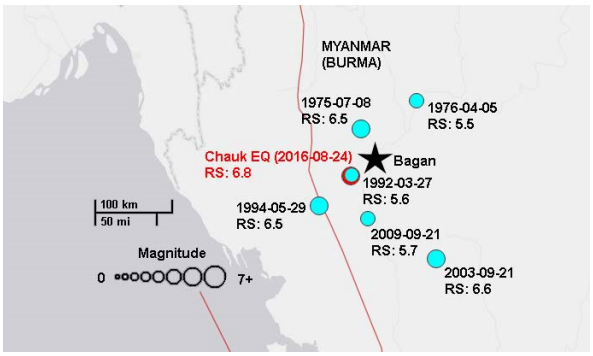

Figure 2: Location of the last strong seismic events (1975 – 2016). RS=Richter scale [20].

Earthquake. Loka temple presents moderate damage at the connection between the two orthogonal walls of the South-East corner, highlighted by two vertical cracks from both the sides. In general, this part suffers more damage than the other portions of the monument and presents also a generalized detachment of the corner along the entire height of the temple. It is important to underline that this damage located at South-East corner was already noticed by Pichard [19] after Bagan Earthquake in 1975 and was yet present before the application of reinforced concrete beams. In other parts of the structure, there are many minor and medium cracks along the boundaries between beams and masonry surfaces. This kind of openings can be associated to the incompatibility of the two materials in terms of stiffness, strength and thermal effects. The tympanum of the North façade is visibly affected by out-of-plane deformations and some parts of this element have been reattached more recently, by using cement based mortar (Fig 3). Due to the orientation of the bricks on the vaulted systems, both in the antechamber and the entrance, there is a longitudinal crack along the length of the vaults. As

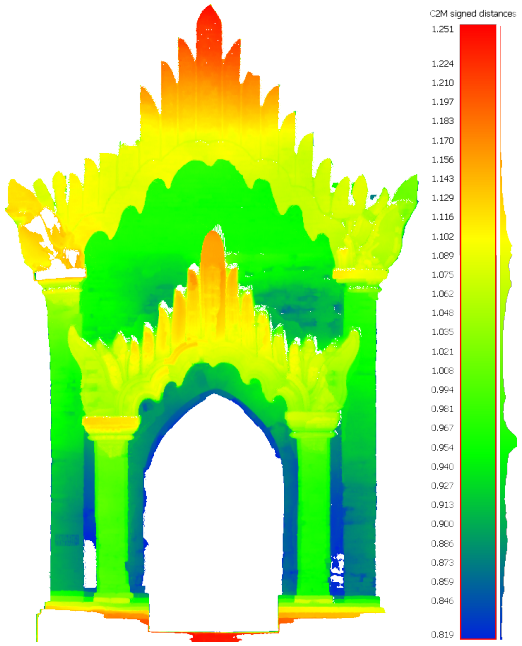

Figure 3: Out-of-plane deformations on the front façade tympanum. C2M distances are computed from a vertical plane fitted on the horizontal profile of the façade.

previously referred, the temple was covered by carvings and stuccoes, which nowadays suffer of heavy decay and damage. All the structure is affected by partial and sometimes complete detachment of the plaster. Moreover, due to the weathering, the original mud mortar disappeared and this caused a widespread disconnection of the brick units. Figure 8 shows the damage pattern of the South façade according to the ICOMOS-ISCS 2008 procedures [24]. The current state of damage have been drawn on the ortho-projection of the coloured point clouds from the 2016 and 2018 surveys.

4.3. Sonic tests

Indirect sonic tests were carried out along all the external surface of the walls, at different heights, on surfaces composed both by original and modern bricks. Direct sonic tests were performed only close the North façade of the temple, because the cross section of the walls in this location is visible and accessible. The sonic tests were performed in-situ during the technical visit in May 2018, using an impulse hammer PCB, a piezoelectric accelerometer PCB ($\pm 0.5\,g$) and an acquisition board NI USB 4431. The tests were repeated more than 30 times per each location (17 locations of measurement along the structure) to give statistical stability to the results. From the Equation 1, Young's modulus (E) can be estimated as function of the density of the material ($\rho = 1777\ kg/m^3$) [21], Poisson's ratio ($\nu = 0.2$) and the velocity of the waves ($VP = 280 - 310\ m/s$) [25].

$$E = \frac{\rho V_p^2 (1+\nu)(1-2\nu)}{(1-\nu)} \tag{1}$$

4.4. LiDAR survey

Two different metric surveys of the temple were performed using a Terrestrial Laser Scanner (TLS) [2] [3]: in the 2016, before the Chauk earthquake and in 2018, after the event. In 2018 a small traverse was established in the area of the temple. Traversing was essential for aligning the exteriors and interiors point cloud and for checking, with a different technique, the errors in laser scans registration. The position of the benchmarks was indeed set in order to measure a set of natural features and targets on the building exteriors and interiors to be used as GCPs[4]. Table 1 shows the residuals on the benchmarks coordinates [5].

The LiDAR surveys performed in 2016 and 2018 covered all the exterior façades and the interiors of the temple. Figure 1 shows the position of the scans of the 2018 survey: a loop scheme was set for the exteriors while the scans from the interiors follow linear sequence, from the antechamber to the main room. A similar approach was used for the 2016 survey. Figure 4 shows the point spacing of the registered point clouds, computed with Meshlab [26] as the average distance from each point to his neighbours. Datasets from 2018 survey are a bit denser, especially regarding the exteriors, because the number of scan was doubled from 9 scans in 2016 to 18 scans in 2018, while for the interiors the number was almost the same (6 scans in 2016 and 7 in 2018). The sparser dataset (2016 exteriors) has 95% of the samples with a point spacing between 2 and $8\,mm$. Figure 5 shows that, apart from the small differences within the surveys, uncertainty deriving from point clouds roughness is below $8\,mm$ for 95% of the sampled data in the worst scenario (2016 exteriors). These point cloud statistics show a potential tolerance of the metric information being extracted from the data in line with the goal to detect spatial changes of $1\,cm$ size (or bigger). 9-Point clouds were re-sampled in order to reduce the point cloud density. Points closer one to each other

Station point	**X** (mm)	**Y** (mm)	**Z** (mm)
2000	0	0	0
4000	0	2	9
1000	2	3	11
3000	2	3	11
5000	5	1	13

Table 1: Traverse residuals on the benchmark coordinates. 2000 was set as the origin of the system.

[2] TLS is a subset of the LiDAR technology targeted to building surveying. Their range is within some meters to few hundreds of meters and they are also usually equipped with a low-res camera whose pictures are used for colouring the point cloud

[3] A FARO Focus 3D X330 was used, with an angular accuracy of 19", a ranging error (tolerance) of $\pm 2\,mm$ and noise between 0.3 and $0.4\,mm$.

[4] A Leica TS11 Total Station (TS) was used, with an angular accuracy of 3" and a distance accuracy of $1\,mm + 1.5\,ppm$ with standard prism and $2\,mm + 2\,ppm$ reflectorless.

[5] Traverse adjustment were performed with the Least Squares (LS) method using the Microsurvey Starnet software.

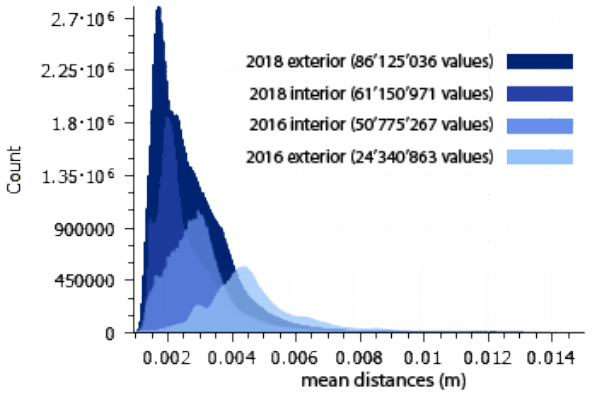

Figure 4: Point clouds densities. X axis show the average distances between points (m) and Y axis the values count (number of points for each point spacing value).

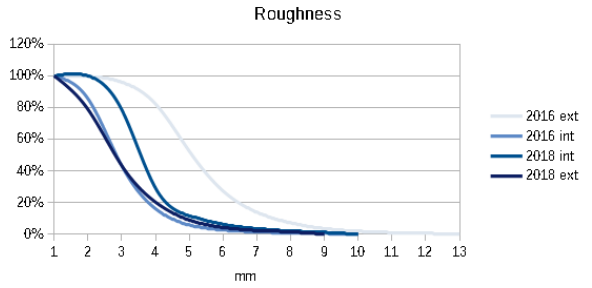

Figure 5: Point clouds roughness. X axis shows the distances and Y axis the percentage of points with that roughness value. Point clouds roughness is calculated as a distance $\pm d$ from each point to a plane fitted on his neighbours within a radius $r = d$.

more than $1\,mm$ were filtered out. Additionally sparse points were also removed before the registration in order to reduce the possible influence of different point cloud densities in the registration [6]. Table 2 shows the residuals and the statistics for the scans co-registration. Scans from the interiors, all placed along the longitudinal axis and featured by high overlap, were co-registered incrementally using the ICP implementation in CloudCompare [7]. Overlapping percentage among the scans from the exteriors was significantly lower, occurring only between adjacent pairs. Consequently different registration approaches were chosen for the exteriors: in 2016 markers were placed on the scene so co-registration was target-based, while the 2018 scans were registered automatically using a global co-registration approach implemented in Scene [8].

Point cloud	**RMSE** (mm)	**Overlap** (%)	**Scan points** (M)
2016 int.	4.3	82%	59
2016 ext.	2.8	57%	24
2018 int.	3.0	91%	84
2018 ext.	2.3	59%	120

Table 2: Co-registration statistics. For each co-registration the mean values for the residuals, the pairs overlap and the total number of points are shown. The registration of the 2016 exteriors was target-based.

4.5. Deformation analysis

To avoid any bias that could affect the results of deformation analysis, a set of tie points placed on the basement and the floor of the temple were manually identified as stable areas for the exteriors and interiors registration respectively. The main purpose of this deformation analysis was indeed to detect and quantify the permanent relative movements of the structural elements due to the Chauk earthquake, while the absolute movements of the entire building were out of the scope of this research. Tie points were measured on the 2018 point clouds which have been registered on a set of GCPs, independently measured with the total station from the traverse benchmarks. Table 3 shows the residuals for the 2018 survey registration with GCPs and the registration of the 2016 point cloud on the 2018 one, using the selected tie points. Two tests were conducted using the C2M and M3C2 methods. They were chosen because both have been

Point cloud	**RMSE** (mm)	**Points**
2018 int. - GCPs	2.5	5
2018 ext. - GCPs	4.6	6
2016 - 2018 ext.	3.2	5
2016 - 2018 int.	3.3	4

Table 3: Residuals on the GCPs used for the 2018 survey registration and tie points for the alignment with the pre-earthquake one.

[6] The filter employed calculates the standard deviation of the mean distances from a point to his neighbours and rejects points with higher values.

[7] `https://www.danielgm.net/cc/`

[8] `https://www.faro.com`.

proven to be less influenced by point cloud roughness and spatial density, both allowing the calculation of the signed distance, while the C2C methods usually gives only an absolute value as result. The signed distance computation is quite relevant in structural monitoring as it can be used to qualify the kind of deformation occurred. The surface reconstruction was performed using the Screened Poisson method, which is a very popular approach for surface reconstruction [27, 28]. The algorithm requires the computation of normals, whose direction is consistent for all the point set. Given the regular shape of the object normals estimation was performed separately with a new innovative approach and the same data used for the two comparisons [29]. The chosen method uses the Hough Transform technique [9] to detect the edges [32] and a Convolutional Neural Network (CNN) [10] to learn the parameters of the function mapping the normals, basing on the point cloud features, like density, outliers and noise. The method is very effective for application to sharp-edged surfaces and large point cloud data sets. Three tests were performed to choose the meshing level of accuracy, using the spatial sampling of the octree structure. Table 4 shows the statistics from the meshing process of the 2018 exteriors point cloud. Starting from an octree cell with a 6 mm side at level 12, the noise from different scans point spacing was becoming visible, so level 11, with a 12 mm cell was chosen. For all the tests the denser point clouds from the 2018 survey were chosen as reference, while the 2016 survey was the compared one, to avoid any possible error due to a different spatial sampling between the two sets. Different spatial samplings within the survey scans and within the single scans were addressed during the co-registration step with a statistical filter(see subsection 4.4).

5. Results and Discussion

Table 5 summarizes the main parameters involved and obtained from the tests performed on the masonry walls. The results of sonic tests allowed to estimate that the average Young's modulus of the masonry walls of the temple is equal 0.46 GPa, in which the highest value is 1.1 GPa (recent masonry with cement based mortar) and the lowest value is 0.25 GPa (deteriorated original masonry). The lowest value, corresponding to the most damaged part of the structure detected by the damage survey (Figure 8), has been discarded.

Octree level	**Side size** (mm)	**Triangles** (M)
11	12	13
12	6	35
13	3	139

Table 4: Statistics of the 2018 exterior point cloud meshing. 86M of points were sampled to build the surface

Mechanical properties for the masonry

Samples	**E** [GPa]	**V** $[m/s]$	$\boldsymbol{\rho}$ $[Kg/m^3]$	$\boldsymbol{\nu}$ $[-]$
Direct tests	0.41	∼280.0	1777	0.2
Indirect tests	0.50	∼310.0	1777	0.2

Table 5: Summary of sonic testing results

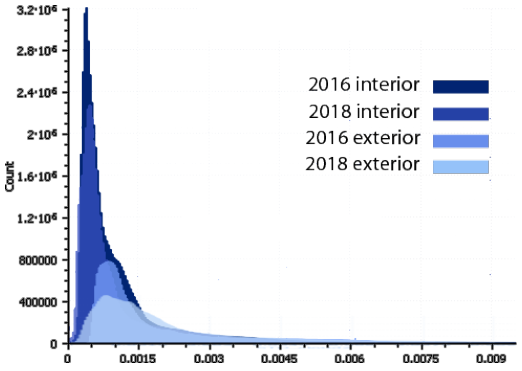

Figure 6: Standard deviations of the point clouds used for the comparison test with the M3C2 method (search radius $r = 2\,cm$). Values show the deviation of the points from the tangent plane computed locally from the normals.

Point clouds comparison with the M3C2 method test was performed with a maximum distance for correspondences search chosen to avoid false positive results due to the highly detailed wall surfaces

[9] The Hough Transform [30, 31], originally developed to detect simple features in 2D space, was later extended to detect any arbitrary feature in the 2D and 3D space and is widely used technique in several Computer Vision applications.

[10] CNNs are multilayered Artificial Neural Networks (ANNs) widely used to solve machine learning and data mining problems, ANNs are computing systems inspired by the functioning of neural networks in the animals brain.

of the temple. Although the presence of holes in one of the two cloud is computed by the M3C2 algorithm as an undefined value, the presence of other points, belonging to other parallel portions of the surface, can result in a false correspondence if it is within the search distance limit. Thus the limit for the search distance was set to a value of 10 cm so that two parallel surfaces would not have been intersected along the normal direction. A different test was conducted to determine the best radius for the correspondence search within the tangent plane. Results of the test on the search radius are summarized in the figure 7 and indicate that for radii $> 2\,cm$ the maximum uncertainty is $\sim 10\,mm$ while for smaller values it increases to $\sim 30mm$, so that almost all the deformations in that area are undetectable. Figure 6 shows the standard deviation distribution across the point clouds used for the test.

Figure 10 shows a map of the deformations occurred in the interiors measured with the M3C2 method. Here the main deformations are in the main room, where small portions of the wall coating, up to 4 cm thickness, detached after 2016. In figure 9 results of the exteriors comparison on the front façade performed with both the methods (C2M and M3C2) are shown. In the exteriors the main significant changes occurred in the upper par of the tympanum which tilted forward after the 2016 earthquake. At the top of the tympanum the measured displacement along the perpendicular direction was of thereabout 3 cm.

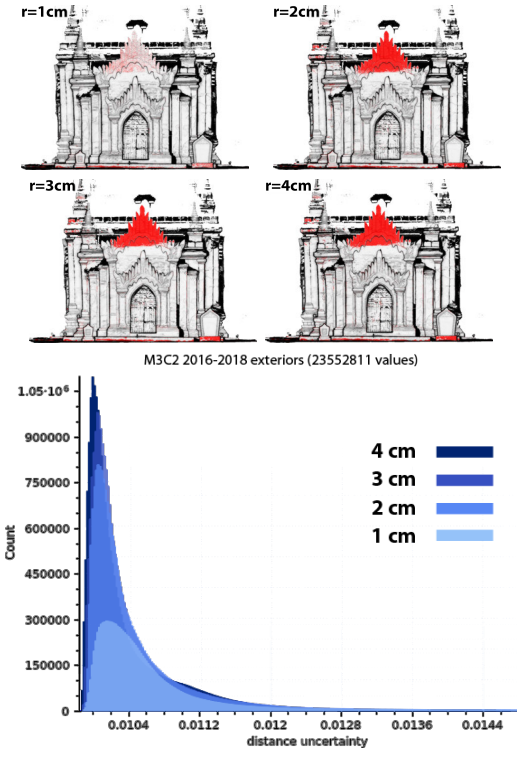

Figure 7: Distance uncertainties on the same M3C2 comparison tested with different search radius values and the effect on significant changes detection in the front façade (red points).

Although a comprehensive comparison of the different algorithms for point clouds comparison was out of the scope of the present paper, the test conducted on the exteriors show significant differences between the results of the C2M and M3C2 analyses. As expected they both show a similar deformation on the upper part of the tympanum in the front façade, however preliminary results of the tests indicate the C2M method has potentially bigger uncertainties. Indeed table 6 shows the standard deviation is about two times bigger with the C2M method.

C2C test	**SD** (mm)
C2M exteriors	24
M3C2 exteriors	10
M3C2 interiors	7

Table 6: Standard deviation of the values distribution from the exteriors, compared with the C2M and M3C2 methods.

6. Conclusions

This paper presents a study on advanced non-destructive techniques for the conservation of historic buildings. The Loka-Hteik-Pan temple (Bagan, Myanmar) was adopted and the application of the techniques was evaluated. The damage survey allowed to conclude that temple presents moderate damage, highlighted by the cracks in the South-East corner and the out-of-plane deformation of the tympanum of the North façade. The sonic tests allowed to identify the different types of masonry of the structure and estimate theirs Young's moduli.

The deformation analysis with the TLS data has proven to be effective for detecting changes of 1 cm size or bigger. Moreover the M3C2 method used for distances computation is the more accurate available at the moment because it takes into account

all the error components, providing reliable results. Relatively small deformations and material losses can be efficiently detected and measured. Accuracy and efficiency can be improved with the use of a fixed set of GCPs placed outside the area where deformations are to be searched, independently measured and adjusted at each epoch. This GCPs network can be used exclusively for the registration of the surveys acquired in different times, while other sets of GCPs are used, if necessary, to register the scans acquired within the same period. This technique is also more precise as avoid the propagation of registration errors through the different surveys [13]. With this improvement portions of the building which are marked as being affected by deformations can be checked efficiently and quickly with high precision without the need to survey the whole building at each time. Furthermore the detachments and deformations analysis can also be efficiently performed on site, allowing its results together with those of the visual inspection to be used for guiding the sonic tests to be performed on the structure.

7. Acknowledgements

The authors wish to acknowledge Dr. U Kyaw Oo Lwin Director General of the Department of Archaeology and National Museum, Dr. Sint Soe, Rector of Mandalay Technological University and Mrs. Ohmar Myo of UNESCO Myanmar for this unique opportunity to collaborate in the conservation of built heritage in Bagan, Myanmar. Other thanks go to all the students that participated in the documentation workshop from Mandalay Technological University, Department of Archaeology and Carleton University.
Furthermore, the authors would like to acknowledge the outstanding support staff of Carleton Immersive Media Studio (CIMS). Finally, we would like to thank all the individuals and institutions that helped with the completion of this article.

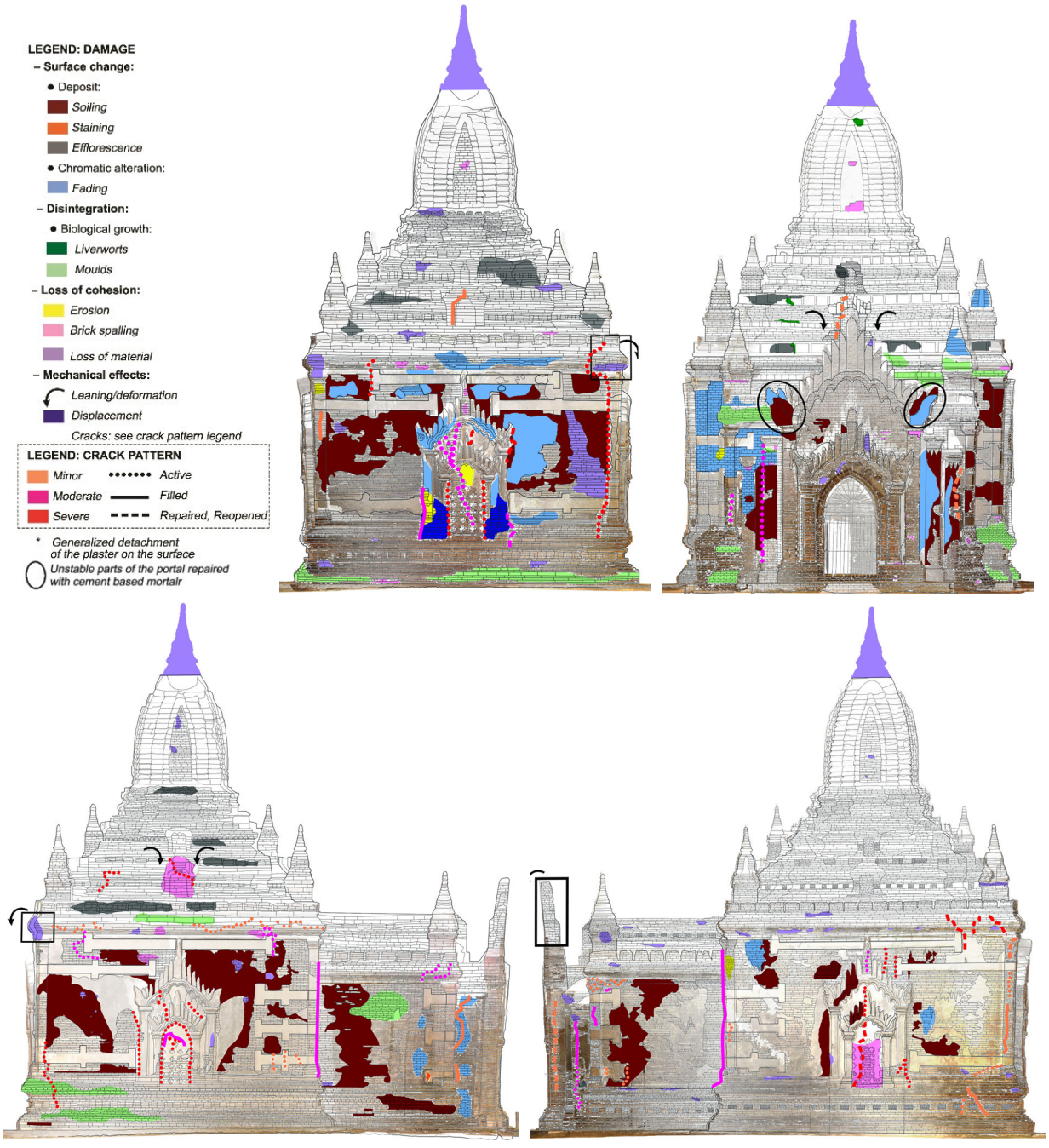

Figure 8: Deterioration mapping on the building elevations superimposed on the coloured point clouds from the 2018 survey.

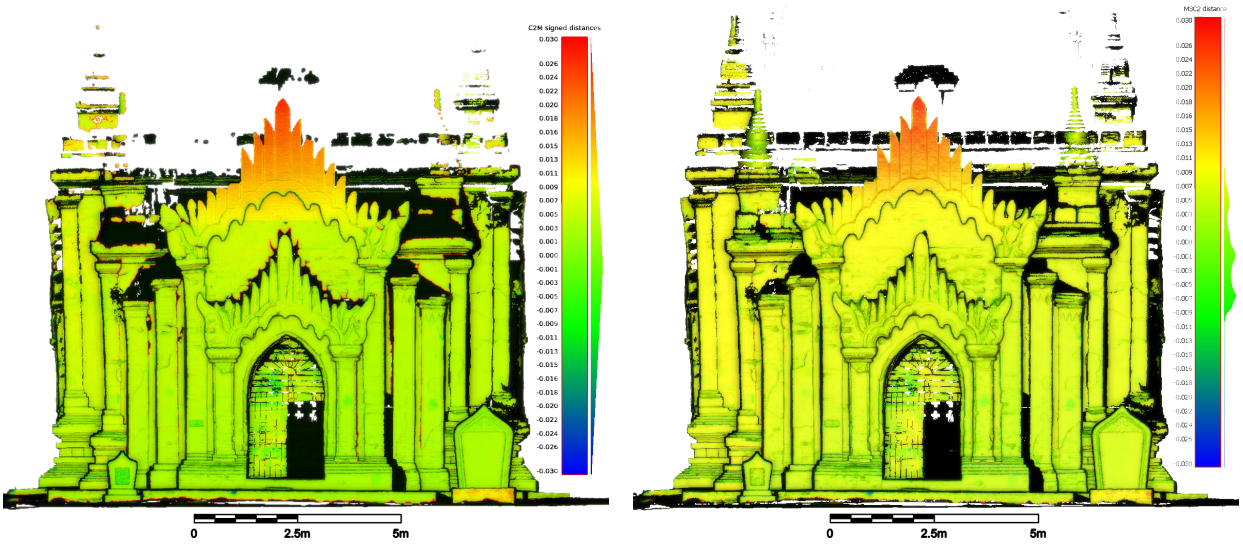

Figure 9: C2M (left) and M3C2 (right) exteriors comparisons, front view. Scale bar spans from -30 to $+30\,mm$. On its right the distribution of the sample. Significant changes correspond to a forward movement of the upper part of the tympanum.

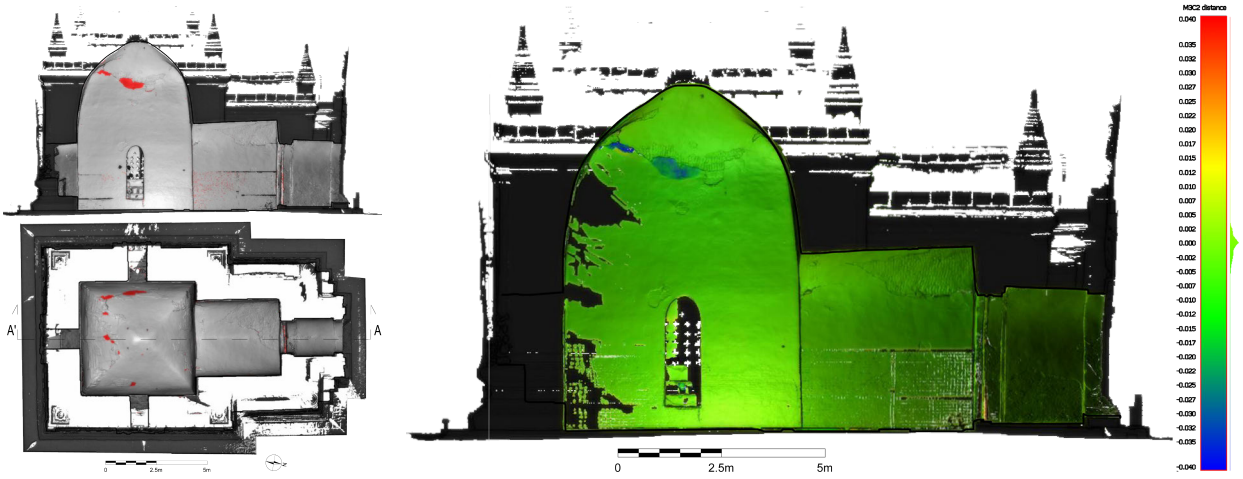

Figure 10: M3C2 interiors comparison, vertical section. Scale bar spans from -40 to $+40\,mm$, on its right the distribution of the sample. Changes bigger than uncertainties are highlighted in red and correspond to plaster detachments in the main chamber vault. Outliers are visible in the lower portion of the antechamber (due to the barriers) and the door between the entrance and the antechamber.

References

[1] ICOMOS, Principles for the Analysis, Conservation and Structural Restoration of Architectural Heritage, 2003.

[2] RecorDIM (for Heritage Recording, Documentation and Information Management) - Task Group 16 Draft report, CIPA - International Committee for Documentation of Cultural Heritage, 2007.

[3] J. Shan, C. Toth, Topographic Laser Ranging and Scanning: Principles and Processing, Second Edition, Taylor & Francis, 2018.

[4] A. Pesci, G. Casula, E. Boschi, Laser scanning the Garisenda and Asinelli Towers in Bologna (Italy): Detailed Deformation Patterns of Two Ancient Leaning Buildings, Journal of Cultural Heritage 12 (2011) 117–127.

[5] L. Bornaz, F. Rinaudo, Terrestrial Laser Scanner Data Processing 35 (2004).

[6] H. Freeman, D. J. Meagher, Octrees: A data structure for solid-object modeling, in: H. Freeman, G. G. Pieroni (Eds.), Computer Architectures for Spatially Distributed Data, Springer Berlin Heidelberg, Berlin, Heidelberg, 1985, pp. 249–259.

[7] P. J. Besl, N. D. McKay, A Method for Registration of 3-D Shapes, IEEE Transactions on Pattern Analysis and Machine Intelligence 14 (1992) 239–256.

[8] D. Wujanz, D. Krueger, F. Neitzel, Defo Scan++: Surface Based Registration of Terrestrial Laser Scans for Deformation Monitoring, Joint International Conference on Deformation Monitoring, 2013.

[9] D. Wujanz, D. Krueger, F. Neitzel, Identification of Stable Areas in Unreferenced Laser Scans for Deformation Measurement, The Photogrammetric Record 31 (2016).

[10] A. Pesci, G. Teza, E. Bonali, G. Casula, E. Boschi, A Laser Scanning-Based Method for Fast Estimation of Seismic-Induced Building Deformations, ISPRS Journal of Photogrammetry and Remote Sensing 79 (2013) 185–198.

[11] I. Puente, R. Lindenbergh, A. Van Natijne, R. Esposito, R. Schipper, Monitoring Of Progressive Damage in Buildings Using Laser Scan Data, in: ISPRS - International Archives of the Photogrammetry, Remote Sensing and Spatial Information Sciences, volume 42, 2018, pp. 923–929.

[12] P. Cignoni, C. Rocchini, R. Scopigno, METRO: Measuring Error on Simplified Surfaces, Computer Graphics Forum 17 (1998) 167–174.

[13] D. Girardeau-Montaut, M. Roux, R. Marc, G. Thibault, Change Detection on Points Cloud Data Acquired with a Ground Laser Scanner, 2005.

[14] D. Lague, N. Brodu, J. Leroux, Accurate 3D Comparison of Complex Topography with Terrestrial Laser Scanner: Application to the Rangitikei Canyon (N-Z), ISPRS Journal of Photogrammetry and Remote Sensing 82 (2013) 10–26.

[15] E. Widyaningrum, B. Gorte, Comprehensive Comparison of Two Image-Based Point Clouds from Aerial Photos with Airborne Lidar for Large-Scale Mapping, in: ISPRS - International Archives of the Photogrammetry, Remote Sensing and Spatial Information Sciences, volume 42, 2017.

[16] T. Barnhart, B. Crosby, Comparing Two Methods of Surface Change Detection on an Evolving Thermokarst Using High-Temporal-Frequency Terrestrial Laser Scanning, Selawik River, Alaska, Remote Sensing, vol. 5, issue 6, pp. 2813-2837 5 (2013) 2813–2837.

[17] A. Gruen, D. Akca, Least Squares 3D Surface and Curve Matching, ISPRS Journal of Photogrammetry and Remote Sensing 59 (2005) 151–174.

[18] O. Monserrat, M. Crosetto, Deformation Measurement Using Terrestrial Laser Scanning Data and Least Squares 3D Surface Matching, ISPRS Journal of Photogrammetry and Remote Sensing 63 (2008) 142–154.

[19] P. Pichard, Inventory of Monuments at Pagan, Bangkok, 1991.

[20] H. Aung, Myanmar Earthquakes History (3rd Edition, August, 2017), 2017.

[21] D. Mezzino, Cultural Built Heritage's Tangible and Intangible Dimensions and Digitalization Challenges, Ph.D. thesis, Carleton University, 2017.

[22] D. Mezzino, L. Chan, M. Santana Quintero, M. Esponda, S. Lee, A. Min, M. Pwint, Built Heritage Documentation And Management: an Integrated Conservation Approach in Bagan, ISPRS Annals of Photogrammetry, Remote Sensing and Spatial Information Sciences 4 (2017) 143–150.

[23] D. Mezzino, M. Esponda, M. Santana Quintero, Myanmar. Architectural Documentation of Historic Temples, 2017.

[24] ICOMOS-ISCS (Ed.), Illustrated Glossary on Stone Deterioration Patterns, Champigny Marne, 2008.

[25] L. Miranda, J. a. Rio, J. a. Guedes, A. Costa, Sonic Impact - Method A New Technique for Characterization of Stone Masonry Walls, Construction and Building Materials 36 (2012) 27–35.

[26] P. Cignoni, M. Callieri, M. Corsini, M. Dellepiane, F. Ganovelli, G. Ranzuglia, MeshLab: an Open-Source Mesh Processing Tool, in: V. Scarano, R. D. Chiara, U. Erra (Eds.), Eurographics Italian Chapter Conference, The Eurographics Association, 2008.

[27] M. Kazhdan, M. Bolitho, H. Hoppe, Poisson Surface Reconstruction, in: Proceedings of the Fourth Eurographics Symposium on Geometry Processing, SGP '06, Eurographics Association, Switzerland, 2006, pp. 61–70.

[28] M. Kazhdan, H. Hoppe, Screened Poisson Surface Reconstruction, ACM Trans. Graph. 32 (2013) 29:1–29:13.

[29] A. Boulch, R. Marlet, Deep Learning for Robust Normal Estimation in Unstructured Point Clouds, Computer Graphics Forum (2016).

[30] R. O. Duda, P. E. Hart, Use of the Hough Transformation to Detect Lines and Curves in Pictures, Commun. ACM 15 (1972) 11–15.

[31] D. Ballard, Generalizing the Hough Transform to Detect Arbitrary Shapes, Pattern Recognition 13 (1981) 111 – 122.

[32] A. Boulch, R. Marlet, Fast Normal Estimation for Point Clouds with Sharp Features using a Robust Randomized Hough Transform, Computer Graphics Forum 31 (2012) 1765–1774.